

TWO-XRD-LINE FERRIHYDRITE AND Fe–Si–Mn OXYHYDROXIDE MINERALIZATION FROM FRANKLIN SEAMOUNT, WESTERN WOODLARK BASIN, PAPUA NEW GUINEA

TREVOR BOYD* AND STEVEN D. SCOTT

Department of Geology, University of Toronto, 22 Russell Street, Toronto, Ontario M5S 3B1, Canada

ABSTRACT

Large deposits of Fe–Si–Mn oxyhydroxide, intimately associated with active warm springs, cover the flanks and caldera of Franklin Seamount in the western Woodlark Basin, Papua New Guinea. The deposits are dominated by poorly crystalline Fe oxyhydroxide, so-called two-XRD-line ferrihydrite. Data on hydrothermal samples of ferrihydrite from Franklin Seamount provide new insights into the atomic structure and chemical composition of this mineral. Electron microscopy supported by X-ray and selected-area electron-diffraction (XRD, SAED) analysis shows that the Franklin Seamount ferrihydrite consists of soft friable agglomerates of randomly stacked colloidal platelets or crystallites, 20–90 Å in diameter, which possess short-range atomic order in two dimensions and highly variable specific surface-areas. Differential thermal analysis indicates that the ferrihydrite is very stable, not transforming to hematite until 570°C. Semiquantitative energy-dispersion spectroscopy (EDS) analysis with a spatial resolution of 35 Å indicates that agglomerates of pure ferrihydrite contain important amounts of Si (on average, 7.5 wt.% Si) and a constant Si:Fe ratio (on average, 0.45, atomic proportions) plus minor but variable amounts of sorbed P, S and As. Individual crystallites exhibit very little beam-induced damage during the EDS analysis. We suggest that Si is capable of being incorporated within the structure of the ferrihydrite. This suggestion is supported by XRD patterns showing a significant shift in the 11 (*hk*) hump to higher values of *d*, compared to Si-free ferrihydrite, and by the thermal stability of the mineral. EDS results and results of bulk analyses demonstrate the wide range of compositions of two-XRD-line ferrihydrite; nevertheless, an average composition of $V^{1}(\text{Fe})_{2.9}^{\text{IV}}(\text{Si, Fe, Al})_{1.3}(\text{O, OH, H}_2\text{O})_{12}$ is proposed for the samples from Franklin Seamount.

Keywords: ferrihydrite, crystal structure, sorption, iron, silicon, X-ray powder diffraction, transmission electron microscopy, thermal analysis, Franklin Seamount, Papua New Guinea.

SOMMAIRE

Des gisements importants d'un oxyhydroxyde de Fe–Si–Mn sont intimement associés aux événements d'eau tiède le long des flancs et de la caldeira du guyot de Franklin, dans la partie occidentale du bassin de Woodlark, en Papouasie-Nouvelle-Guinée. Les gisements contiennent surtout un oxyhydroxyde désordonné de fer que l'on qualifie de ferrihydrite à deux raies (en diffraction X). Les données obtenues sur les échantillons de ferrihydrite hydrothermale du guyot de Franklin permettent de nouvelles interprétations à propos de la structure atomique et la composition chimique de ce minéral. Les observations en microscopie électronique, étayées par des données en diffraction X et diffraction d'électrons sur aire restreinte, montrent que la ferrihydrite du guyot de Franklin est faite d'amas mous, friables et désordonnés de plaquettes ou de cristallites colloïdaux entre 20 et 90 Å de diamètre, possédant un agencement ordonné en deux dimensions et des surfaces spécifiques très variables. Une analyse thermique différentielle prouve que la ferrihydrite est très stable, sans tendance à se transformer en hématite jusqu'à un seuil de 570°C. Une analyse semiquantitative en dispersion d'énergie avec résolution spatiale de 35 Å montre que les agglomérats de ferrihydrite pure contiennent un niveau élevé en Si (7.5% Si, poids, en moyenne) et un rapport Si:Fe constant (0.45, proportion atomique, en moyenne), ainsi que des quantités moindres mais variables de P, S et As adsorbées. Les cristallites individuels ne semblent pas endommagés par le faisceau d'électrons au cours de l'analyse par dispersion d'énergie. À notre avis, le Si serait incorporé dans la structure de la ferrihydrite. Cette hypothèse repose sur le décalage important de la raie floue 11 (*hk*) vers une valeur plus élevée de *d*, par rapport à la ferrihydrite sans Si, et sur la stabilité thermique de ce minéral ainsi substitué. Les résultats de l'analyse en dispersion d'énergie et de l'analyse globale démontrent la grande variabilité en composition de la ferrihydrite à deux raies; dans la région du guyot de Franklin, la composition moyenne de ce minéral serait $V^{1}(\text{Fe})_{2.9}^{\text{IV}}(\text{Si, Fe, Al})_{1.3}(\text{O, OH, H}_2\text{O})_{12}$.

(Traduit par la Rédaction)

Mots-clés: ferrihydrite, structure cristalline, sorption, fer, silicium, diffraction X sur poudre, microscopie électronique par transmission, analyse thermique, guyot de Franklin, Papouasie-Nouvelle-Guinée.

* *Present address:* Millennium Minerals Corp., 350 Cleveland Street, Toronto, Ontario M4S 2W9, Canada. *E-mail address:* trevorb@aracnet.net

INTRODUCTION

Mounds and chimneys of Fe–Si–Mn oxyhydroxides associated with active low-temperature springs intermittently cover the flanks and caldera of a submarine volcano in the western Woodlark Basin, southwest Pacific (Fig. 1). The volcano, informally named Franklin Seamount, straddles a zone of seafloor rifting and passive spreading that is propagating westward into Papua New Guinea (Benes *et al.* 1994). The oxyhydroxide deposits surround and flank two dormant barite-dominant spires that contain up to 21 ppm Au and 505 ppm Ag (Binns *et al.* 1993).

Since 1986, the area has been visited several times by a joint Papua New Guinea – Australia – Canada (PACLARK) research team (Binns & Whitford 1987). In 1990, the seamount was explored with the *Mir* submersible and the *RV Akademik Mstislav Keldysh* during the Soviet Union – Papua New Guinea – Australia – Canada SUPACLARK expedition (Binns *et al.* 1990a, Lisitsin *et al.* 1991). On this expedition, the deposits were closely investigated, and numerous samples of

oxyhydroxide material were recovered during four submersible dives (Binns 1990, Lisitsin *et al.* 1991). Binns *et al.* (1993) and Bogdanov *et al.* (1997) described in detail the geological setting, morphology and internal structure of the oxyhydroxides, structures and textures of the hand samples collected, and postcruise laboratory research completed during the PACLARK – SUPACLARK program. Preliminary investigations reported in Binns *et al.* (1993) and Bogdanov *et al.* (1997) show that the hydrothermal material is dominated by poorly crystalline Fe oxyhydroxide. Nontronite, birnessite, opal-A and possible todorokite and vernadite also were identified.

This research on poorly crystalline Fe oxyhydroxide, or so-called two-XRD-line ferrihydrite, at Franklin Seamount has generated a better understanding of the atomic structure and chemical composition of the mineral. The current investigation was undertaken to better characterize poorly crystalline Fe oxyhydroxide, and to compare this ferrihydrite with similar deposits at other seafloor locations and with ferrihydrite both in surface freshwater environments and synthesized in the labora-

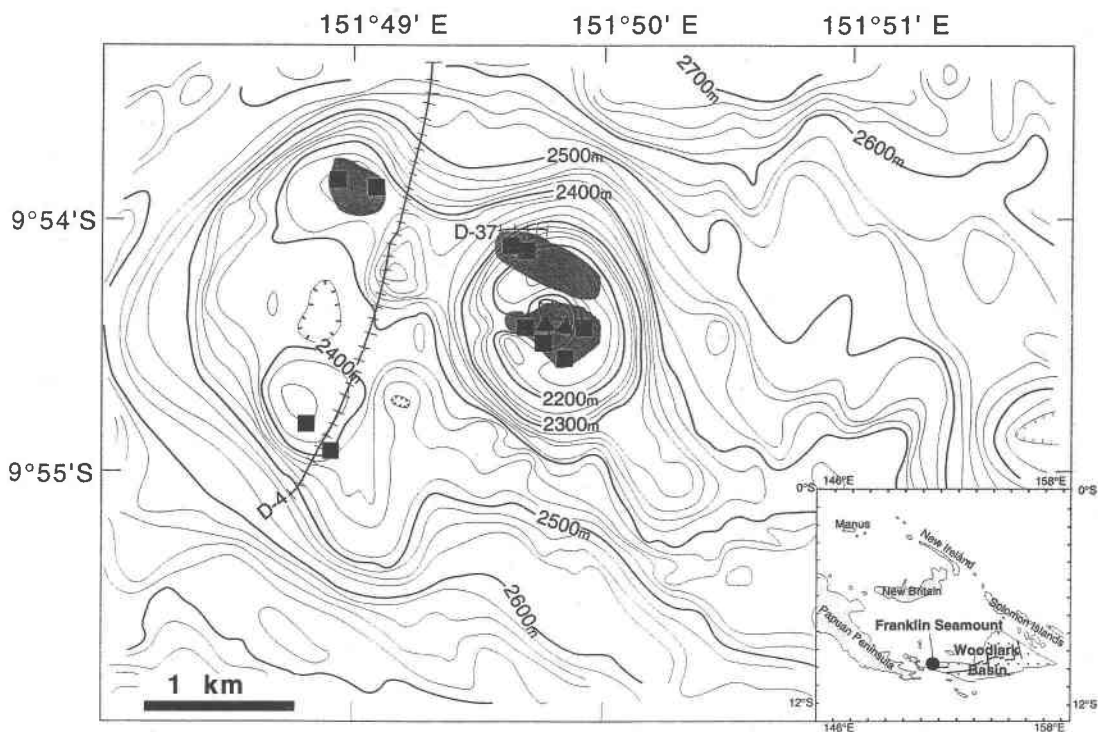


FIG. 1. Distribution of Fe–Si–Mn oxyhydroxide deposits and precious-metal-rich barite spires at Franklin Seamount, western Woodlark Basin, Papua New Guinea. Filled squares are oxyhydroxide sample sites. Filled triangles are locations of barite spires. Shaded areas represent the extent of Fe–Si–Mn oxyhydroxide fields based on submersible dives during the 1990 SUPACLARK expedition. Dashed line marks the approximate track of a dredge from the 1987 PACLARK expedition.

tory. Reviews of ferrihydrite and its atomic structure are found in Eggleton & Fitzpatrick (1988), Waychunas (1991) and Jambor & Dutrizac (1998).

We report the results of mineralogical research on the oxyhydroxides based on bulk geochemistry, X-ray powder diffraction (XRD), scanning electron microscopy – energy-dispersion spectroscopy (SEM–EDS), transmission electron microscopy – energy-dispersion spectroscopy (TEM–EDS) and selected-area electron diffraction (SAED). In addition to these techniques, selected Fe oxyhydroxides were analyzed by high-resolution scanning transmission electron microscopy – energy-dispersion spectroscopy (STEM–EDS) and by thermogravimetric and differential thermal analysis (TGA–DTA) in order to characterize composition, grain size, and short-range crystallographic order in this poorly crystalline material.

METHODS OF INVESTIGATION

The 52 samples were mostly obtained by submersible from chimneys and mounds on the seafloor using a remotely controlled manipulatory arm; others were collected by a shallow (<1 m length) sediment corer attached to the submersible (Binns *et al.* 1993). Once onboard ship, the raw wet samples were put into plastic containers or bags, and were not dried until four months later. Nothing was done to preserve possible organic materials in the samples.

Most of the bulk chemical data were obtained by instrumental neutron activation analysis (INAA). Details of the sample preparation and analytical procedure are discussed in Boyd *et al.* (1993). Boyd *et al.* (1993) and Barnes & Gorton (1984) discussed the precision and accuracy of the INAA technique using the Slowpoke reactor. Some oxyhydroxide samples were sent to a commercial laboratory for whole-rock major- and trace-element analyses by X-ray fluorescence (XRF) on fused glass and pressed pellets, respectively. XRF trace-element analyses on pressed pellets were also conducted at the Université de Montréal. Analyses of standards and duplicate samples by more than one method provided an additional check on the accuracy and precision of the results.

Powdered, randomly oriented air-dried samples were analyzed by XRD, mostly using a Cu-target diffractometer at the Ontario Geological Survey (OGS), Toronto. Where the sample size was too small for standard XRD analysis, small aliquots (<20 mg) were run on a Siemens D–500 Cu-target diffractometer in the Department of Chemistry, University of Toronto. Duplicate samples were run on more than one instrument. An oriented clay fraction of sample M2157–7 was also run on the OGS instrument, then was Mg-glycolated and analyzed again in order to confirm its mineralogy.

A Hitachi H–800 TEM equipped with a Tracor Northern TN–2000 EDS, in the Department of Metallurgy and Materials Science, University of Toronto, was used to study the air-dried samples at high magnifica-

tions (200 kV at 10,000 to 200,000 \times). The EDS analyses were obtained by both spot and raster methods. Some oxyhydroxide samples were examined using a CM12 100 kV Philips TEM and analyzed semiquantitatively with an EDAX PV9900 EDS at the Geological Survey of Japan. A Vacuum Generator HB5 STEM with an attached EDS in the Department of Material Science at McMaster University was also used to analyze some samples. The advantage of this system is its capability for viewing agglomerates at magnifications up to 2 million times with theoretically excellent spatial resolution (0.0035 μm spot size).

DTA–TGA analysis was conducted on sample M292 loc.1 106848 at the Department of Mineralogy of the Royal Ontario Museum to search for changes in temperature and mass that would aid in its identification. XRD analysis indicates the sample consists entirely of poorly crystalline Fe oxyhydroxides.

Semiquantitative compositions from the Tracor Northern TEM–EDS attached to the University of Toronto TEM were obtained by calibrating the integrated element peaks using empirical K-factors derived by the EDS analysis of chlorite, biotite, and garnet electron-microprobe standards. The size of an element peak is strongly dependent on the thickness of the analyzed particle as well as its composition (Peacor 1992, Cliff & Lorimer 1975). In order to overcome this problem, analyses were conducted on sample and standard particles of similar size that obey the thin film criterion, so that analytical inaccuracies due to X-ray absorption and fluorescence could be minimized. Although the degree of influence of these factors is dependent on the composition of the particle (Williams 1984), they generally can be neglected if the particles are less than 0.05 μm thick (Peacor 1992, Cliff & Lorimer 1975).

The calculated error is a measure of the analytical precision of the analysis based on the number of net counts for each element peak as a function of the average peak-to-background ratio of the analyses fitted by Gaussian statistics to two standard deviations (Williams 1984). The data show that although most of the oxyhydroxide samples have compositions different from those of the standards, good semiquantitative analyses are possible. There are, however, significantly higher errors in the data derived from the Hitachi instrument, particularly for the minor elements. As a result, concentrations of P, Ca and Cl are all much higher, and K, S and As are below the detection limit using the older University of Toronto Hitachi instrument compared to data obtained using the newer Philips system at the Geological Survey of Japan.

The theoretical detection-limits of the Hitachi instrument, reached with a calculated error of $\pm 40\%$, can vary with background interference, atomic number of the element, and amount of peak interference due to the sample composition. For the Franklin Seamount samples, detection limits are (in wt.%), 0.8–2.9 for MgO, 1.2–3.5 for Al₂O₃, 0.5–2.0 for SiO₂, 1.1–2.7 for

P₂O₅, 0.9–2.0 for SO₄, 0.3–1.0 for Cl₂O, 0.4–1.1 for K₂O, 0.3–0.9 for CaO, 0.2 for TiO₂, 0.2–2.2 for MnO, 0.2–1.8 for Fe₂O₃, 0.2 for Ni, and 0.1–0.6 for As. Results, not surprisingly, show that the error increases with decreasing element content, which allows for realistic constraints to be placed on interpretation of the data.

The STEM–EDS results were obtained using empirically derived K factors in a similar manner to the TEM–EDS analyses. Errors were calculated similarly, and the values obtained are presented here for sample M2192 loc.1. The compositions are presented as oxides in order to facilitate comparison with the results of TEM–EDS and bulk-chemical analyses. Calculated detection-limits for the STEM–EDS analyses, in wt.%, are 4.0–15 for O, 2.3–5.0 for Mg, 1.2–3.5 for Al, 1.7–5.3 for Si, 1.7–2.7 for P, 1.7–3.8 for Ca, 2.3–7.8 for Mn, and 1.1–5.0 for Fe. This technique has significantly higher detection-limits and lower precision compared to that obtained by the TEM systems. As a result, only semiquantitative estimates for O, Si and Fe were obtained consistently using the STEM–EDS technique. Interpretations of the data are limited by this inaccuracy. Despite the extremely small size and apparent delicate appearance of the agglomerates, as with the TEM–EDS analyses, the agglomerates showed very little degradation when in contact with the analytical beam. In contrast, the chlorite standard of similar size was totally vaporized when analyzed by the beam.

RESULTS

Mineralogy and bulk geochemistry

Bulk compositions of oxyhydroxide samples from Franklin Seamount were previously reported in Binns *et al.* (1993) and Bogdanov *et al.* (1997). These data are discussed here only with reference to their mineralogical characterization. Colors of the dry powdered samples and their XRD identifications of the phase assemblages are summarized in Table 1 and are compared to the bulk geochemistry of similar samples in Table 2; the latter are grouped in terms of Fe-, Fe–Si-, Si-, Mn- and detritus-rich end-members. The analyzed samples have variable amounts of these five end-member types of oxyhydroxides, which is reflected in the wide range of their compositions.

The XRD pattern of the Fe end-member sample (Fig. 2a) shows only a broad hump with a maximum from 2.75 to 2.55 Å, and a very faint secondary hump at approximately 1.5 Å (not shown), indicating the presence of only poorly crystalline oxyhydroxide. This material is “protoferrihydrite”, as named by Bogdanov *et al.* (1997), or two-XRD-line ferrihydrite, a poorly ordered ferric Fe oxyhydroxide described by Carlson & Schwertmann (1981) and Eggleton & Fitzpatrick (1988). It is described by XRD as having a primary hump centered at 2.5 Å and a smaller one at 1.5 Å. These

TABLE 1. DESCRIPTIVE SUMMARY OF THE MINERALOGICAL AND COMPOSITIONAL END-MEMBERS OF 52 SAMPLES OF OXYHYDROXIDE FROM FRANKLIN SEAMOUNT

Sample	GSA Color Chart	Munsul Color	Mineral assemblage based upon XRD analysis
Majority of 52 samples	mostly moderate yellowish brown to dusky yellowish brown	10YR5/4 –10YR2/2	nearly X-ray-amorphous iron oxide predominant; major nontronite and birnessite plus minor amount of opal A. All diluted by variable amounts of volcanic rock and biological detritus
M2192 loc.1 (106848) Fe end-member	moderate brown	5YR4/4	only nearly X-ray-amorphous iron oxide (two-XRD-line ferrihydrite) detected
M2157–7 (106890) Fe–Si end-member	dusky yellow	5Y6/4	only nontronite detected
M2202–2B (106923) Mn end-member	dusky yellowish brown	10YR2/2	dominated by birnessite with trace of iron oxides, nontronite and barite
2202–2–6 (106925) Si end-member	dark yellowish brown	10YR4/2	dominated by opal A with minor nearly X-ray-amorphous iron oxides
106478 D–37 Detritus end-member	pale yellowish brown to grayish	10YR6/2 –10YR7/4	dominated by bottom sediments consisting mostly of local basaltic andesite, terrigenous orange material and biological detritus (volcanic shards, calcite, opal A, feldspar, quartz, dolomite, amphibole and kaolinite)

The GSA and Munsul scales of color are taken from Goddard *et al.* (1948). The detritus end-member refers to the sample whose composition most resembles that of the most common host volcanic rock in the area, Franklin Seamount basaltic andesite. Thus it is interpreted to contain little or no hydrothermal component.

TABLE 2. BULK COMPOSITIONS OF Fe-Si-Mn OXYHYDROXIDES, IN TERMS OF MAJOR AND TRACE ELEMENTS

	Avg.	Range	No.	(1)	(2)	(3)	(4)	(5)
SiO ₂ wt.%	26.1	13.8–64.7	32	14.7	37.5	13.8	64.7	33.0
TiO ₂	0.08	b.d.–0.58	19	0.03	0.06	0.02	0.01	0.58
Fe ₂ O ₃	35.2	10.1–52.9	19	52.9	35.1	27.0	10.1	18.3
Al ₂ O ₃	1.40	0.04–6.45	32	0.09	0.84	0.76	0.09	6.45
MnO	4.86	0.08–25.7	19	2.39	0.16	25.7	1.53	0.45
MgO	1.38	0.50–2.68	32	1.04	1.68	1.42	0.65	2.68
CaO	3.22	0.40–19.7	32	1.33	1.20	0.90	0.40	15.3
K ₂ O	0.86	0.09–1.54	19	0.71	1.32	0.79	0.79	0.67
N a ₂ O	1.85	0.75–2.83	19	1.48	1.83	2.06	1.54	1.82
P ₂ O ₅	1.88	0.53–5.33	19	3.25	1.84	1.36	0.53	0.58
S	0.22	0.09–0.51	23	n.a.	n.a.	n.a.	n.a.	0.18
LOI	23.4	17.5–42.8	19	22.1	17.5	26.0	20.2	20.5
Total	100.2	99.2–100.7		100.2	99.5	100.6	100.7	100.5
Zn ppm	93	b.d.–310	46	91	85	230	67	100
Ni	120	b.d.–540	46	420	b.d.	220	63	80
Co	65	b.d.–270	46	230	5	47	5	24
As	670	10–2900	46	790	170	2100	1900	54
Mo	270	2–2100	46	149	2	770	40	2
Sb	14	1–39	46	10	3	33	39	1
Au (ppb)	32	10–190	46	34	20	320	28	57
Ag	b.d.	b.d.–4	46	b.d.	b.d.	4	b.d.	b.d.
Hg	1	b.d.–5	46	b.d.	1	3	b.d.	b.d.
Ba	380	45–5900	46	139	156	5900	710	240
Cu	64	b.d.–310	24	37	n.a.	31	n.a.	36
Pb	b.d.	b.d.–26	24	b.d.	n.a.	n.a.	n.a.	b.d.

Samples analyzed for the major elements by X-ray fluorescence (XRF) on a fused disk. Samples analyzed for Cu and Pb by XRF on a pressed powder disk. All other data by instrumental neutron-activation analysis (INAA). (1): M2192 loc. 1 (106848), Fe end-member, two-XRD-line ferrihydrite. (2): 106443 D-37, Fe-Si end-member, dominated by nontronite. (3): M2202-2B (106923), Mn end-member, dominated by birnessite. (4): M2202-2-6 (106925), Si end-member, dominated by opal-A. (5): 106478 D-37, detritus-rich local bottom sediment. No.: number of samples analyzed, b.d.: below the limit of detection, n.a.: concentration not determined.

humps represent the 11 and 30 *hk* reflections, respectively. The pattern is indicative of the apparent absence of a third dimension in its short-range structure. The shift of the 2.5 Å hump to higher *d*-values, not dissimilar to the pattern shown in Figure 2a, has been identified for natural Si-rich, two-XRD-line ferrihydrite by Vempati & Loepfert (1989). The color of the Fe-rich end-member sample is like that of the ferrihydrite described by Schwertmann & Cornell (1991). Its composition is similar to natural ferrihydrite in soils and surface springs described in Eggleton (1987), Childs *et al.* (1982) and Carlson & Schwertmann (1981), except that the ferrihydrite from the Franklin Seamount has a significantly higher Si:Fe ratio. On the basis of these results, the name "two-XRD-line ferrihydrite" is used here to describe the poorly crystalline Fe oxyhydroxide at Franklin Seamount.

The XRD pattern of the Fe-Si end-member (Fig. 2b) consists of a series of wide asymmetrical peaks (12.1, 4.53, 3.16, and 2.57 Å) characteristic of a very fine-grained crystalline material like the nontronite from a hydrothermal deposit at Lau Basin (Stoffers *et al.* 1990). The presence of a smectite-group mineral in the sample is demonstrated by the shift of the (001) XRD peak at

12.1 Å to 13.4 Å upon Mg-glycolation. The small shift in the peak is due to the short period of time during which the glycolation was allowed to set (6 hours), rather than to the presence of contamination by a mixed-layer clay, an interpretation supported by the absence of Al (INAA results). A small peak at 1.52 Å (not shown), also noted by Stoffers *et al.* (1990), indicates the dioctahedral structure of the smectite. Although insufficient sample was available for a complete chemical analysis, the bulk composition of another, slightly less pure sample (Table 2) contains dominant Fe and Si, with very low levels of other cations. The XRD patterns, bulk chemical composition, and distinctive khaki color present good evidence for the identification of the Fe-Si end-member as nontronite.

Figure 2c shows the XRD pattern of the most Mn-rich end-member among the oxyhydroxide samples. Contamination by non-Mn-bearing minerals in this sample is indicated by some minor peaks at 4.53 and 3.09 Å, attributed to nontronite and barite, respectively. These identifications are confirmed by analyses indicating that the sample contains significant amounts of Fe, Si and Ba, as well as Mn (Table 2). The remaining peaks (7.11, 3.56, 2.44, and 2.11 Å) all match birnessite, the 7 Å Mn oxyhydroxide. The presence of todorokite, reported by Binns *et al.* (1993), is not confirmed, and may have been misinterpreted by them owing to the collapse of the 10 Å spacing of the mineral to 7 Å in the dried samples (Chukhrov *et al.* 1976). XRD patterns of some of the samples from actively venting chimneys gathered on Franklin Seamount indicate the presence of vernadite, which was also found in local Mn-Fe crusts on basaltic andesite. Vernadite has been widely reported in hydrogenous crusts and nodules (von Stackelberg *et al.* 1990, Giovanoli & Arrhenius 1988).

Figure 2d shows the XRD pattern of the most Si-rich end-member of the oxyhydroxides. The distinctive broad hump centered around 4 Å is consistent with the presence of opal-A (Jones & Segnit 1971). The asymmetric shoulder, at higher angles to the hump, and a weak peak at around 3.1 Å, suggest the presence of two-XRD-line ferrihydrite and a trace of barite, respectively, and are confirmed by the bulk composition (Table 2). Binns *et al.* (1993) reported that some samples have weak humps at 4.2, 2.5–2.7, and 1.7 Å, suggestive of goethite. Similar patterns were found in this study; however, sizes of the humps coincide with compositional variations in a manner consistent with the samples containing variable proportions of opal-A and ferrihydrite.

Results of the XRD analysis indicate significant opal-A in only a few samples (M2202-2-6, M2157-14A, and 106436 D-37). It is possible, however, that other samples contain significant amounts of poorly crystalline silica. Cremer (1994) found for the oxyhydroxide deposits at Loihi Seamount that the XRD pattern of poorly crystalline silica was masked by the presence of Fe oxyhydroxides. The Si attributed to poorly crystalline silica in the Franklin Seamount

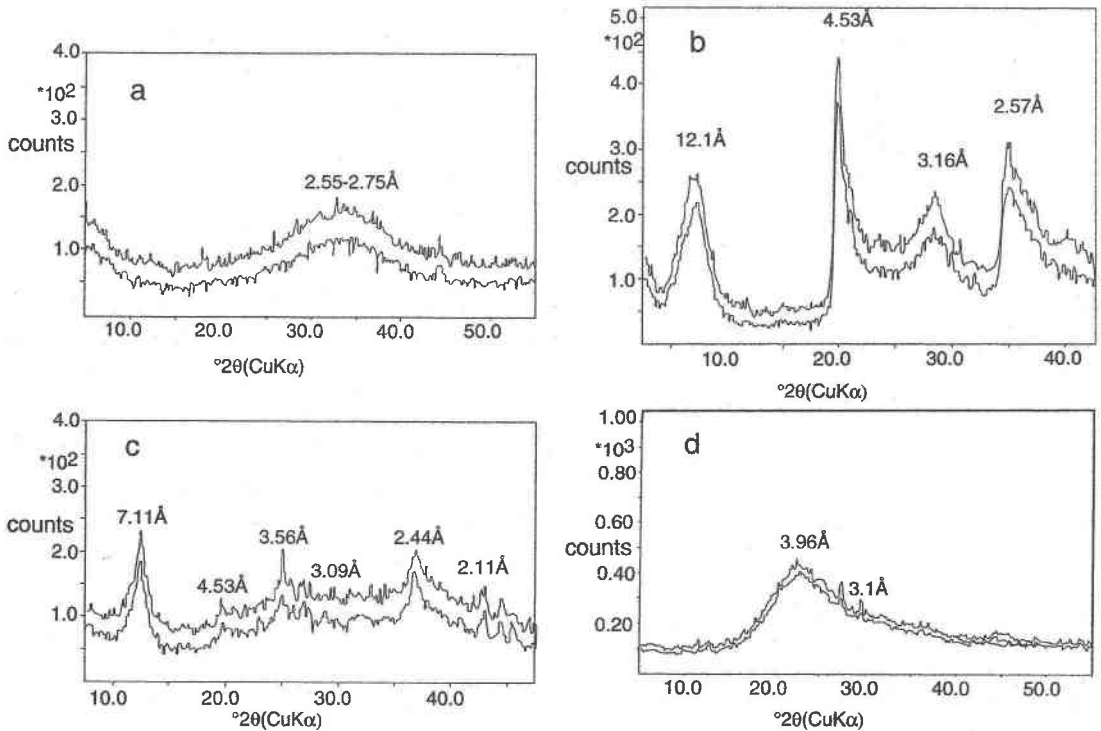


FIG. 2. XRD patterns ($\text{CuK}\alpha$ radiation) of untreated, randomly oriented samples representing the four hydrothermal mineralogical "end-members" at Franklin Seamount. (a) Fe-rich end-member, sample M2192 loc.1 (106848). (b) Fe-Si end-member, sample M2157-7 (106890). (c) Mn-rich end-member, sample M2202-2b (106923). (d) Si-rich end-member, sample 2202-2-6 (106925). Double lines represent upper and lower limits of the XRD traces. The X axis is degrees in 2θ . The Y axis is a qualitative measure of the relative proportion of mineral in sample. Peaks due to halite from the evaporation of seawater have been removed.

samples can be estimated by subtracting the 7.0 wt.% Si content in end-member ferrihydrite from the average recalculated detritus-free Si content of 11.6 wt.% (Boyd 1996). Using this method, the samples contain an average of 4.6 wt.% Si as poorly crystalline silica, although not all of this poorly crystalline silica is necessarily hydrothermal. Fossil debris dominates some samples of bottom sediments around Franklin Seamount, and their XRD patterns show the distinctive opal-A hump similar to that of sample M2202-2-6 from an actively venting chimney.

The mineralogy and major-element geochemistry of the Fe-Si-Mn oxyhydroxides at Franklin Seamount are products of both hydrothermal and detrital components (Boyd *et al.* 1993). The occurrence of these components affects the distribution of trace elements, as does mineralogy, on the basis of the association of the highest As and Mn contents in birnessite and two-XRD-line ferrihydrite and on the overall low trace-element contents in nontronite (Table 2). The high Au, Ag and Ba contents of sample M2202-2-6 record its proximity to

precious-metal-enriched barite spires (Boyd *et al.* 1993), but this may be due to the mechanical incorporation of detrital particles of the barite rather than direct precipitation from hydrothermal fluids. Boyd *et al.* (1993) demonstrated that the high As and Mn and low Zn contents in the Fe-rich samples (Table 2) reflect the ferrihydrite's ability to sorb or coprecipitate such metals if they occur in the hydrothermal environment. The high As and Mo contents of the hydrothermal opal-A rich sample in Table 2 suggest that other poorly crystalline phases are also capable of incorporating these elements.

Thermogravimetric heating of Fe end-member sample M2192 loc.1 106848 gives a smooth and continuous weight-loss of 24% between 40 and 650°C, in reasonable agreement with the 21.1 wt.% loss on ignition (LOI) for this sample (Table 2) and 25 wt.% from the TGA curve for a synthetic two-XRD-line ferrihydrite (Eggleton & Fitzpatrick 1988). DTA of the sample shows a very broad endothermic peak centered at 155°C owing to loss of H_2O and a single broad exothermic peak at 544°C. The width of the latter peak at

half its height is 40°C. This is unlike the curve given by Eggleton & Fitzpatrick (1988), who described synthetic ferrihydrite as having two strong exothermic peaks at 340–355°C and 449°C.

The end-product of the TGA–DTA experiment in this study was hematite with minor quartz. MacKenzie & Berggren (1970) reported the same end-product, and noted that the exothermic peak represents the nucleation and growth of hematite. Another aliquot of the Fe end-member sample heated by DTA to only 400°C has the same poorly crystalline XRD pattern as the unheated material. An additional aliquot of the sample, heated in an open oven to 520°C and then held at that temperature for 5 days, also has the same poorly crystalline XRD pattern, indicating the thermal stability of the mineral. Although maghemite was reported to be produced by Eggleton & Fitzpatrick (1988) as a result of heating synthetic ferrihydrite to a temperature between the two exothermic peaks, Campbell *et al.* (1997) found, for similar experiments, that maghemite formed only in the presence of organic matter, which acted as a reductant. The presence of two exothermic peaks was found not to have a bearing on the presence or absence of maghemite. Particle-size differences may also affect DTA curves; magnetite particles <300 nm in diameter oxidize to hematite through maghemite, whereas magnetite particles >550 nm transform directly to hematite (MacKenzie & Berggren 1970). No indication of the transitional presence of maghemite was found in the heated products of M2192 loc.1, consistent with the paucity of organic material in the samples from Franklin Seamount.

According to Carlson & Schwertmann (1981), the exothermic peak of synthetic ferrihydrite increases from 331 to 778°C with an increase in Si content from 0 to 4.9 wt.%. The Si promotes thermal stability of the material, delaying its transformation to hematite until higher temperatures, and thus bypassing the transitional maghemite phase. Cornell *et al.* (1987) found that both Si and P tend to stabilize synthetic ferrihydrite and retard its transformation to goethite and hematite. The Franklin Seamount ferrihydrite contains high concentrations of Si and P (Tables 2, 3), which likely explains its high-temperature exotherm.

Spot geochemistry and microtextures

The SEM–EDS study of the samples provided a qualitative overview of compositions and microstructures in the samples in preparation for the high-magnification examination and analysis with the TEM system. The filamentous textures that are abundant in many of the samples appear to be of bacterial origin. The remains of bacteria include the recognizable genera *Gallionella*, *Leptothrix* and *Sphaerotilis* (Boyd 1996, see also Bogdanov *et al.* 1997). However, the Fe-rich forms in both active and dormant chimneys also occur as irregularly shaped granular orbs or with no discernible form, and thus is probably non-bacterial (Boyd 1996). Hydro-

thermal poorly crystalline silica locally encases filaments or forms discrete blebs interstitial to the Fe-rich forms, as noted by Juniper & Fouquet (1988) from various hydrothermal deposits of Fe oxyhydroxide in the Pacific Basin. Fossil biogenic debris that consists wholly of silica occurs in some samples. Birnessite, forming rosettes 10 µm in diameter, mostly drapes the Fe oxyhydroxides, indicating that it precipitated later. Nontronite occurs as orthogonal arrays of platelets commonly in the core of samples.

Table 3 gives results of semiquantitative TEM–EDS analyses of typical <2 µm agglomerates of sample M2192 loc.1 106848, together with the bulk geochemistry. TEM images of microtextures of various types of oxyhydroxides are shown in Figure 3.

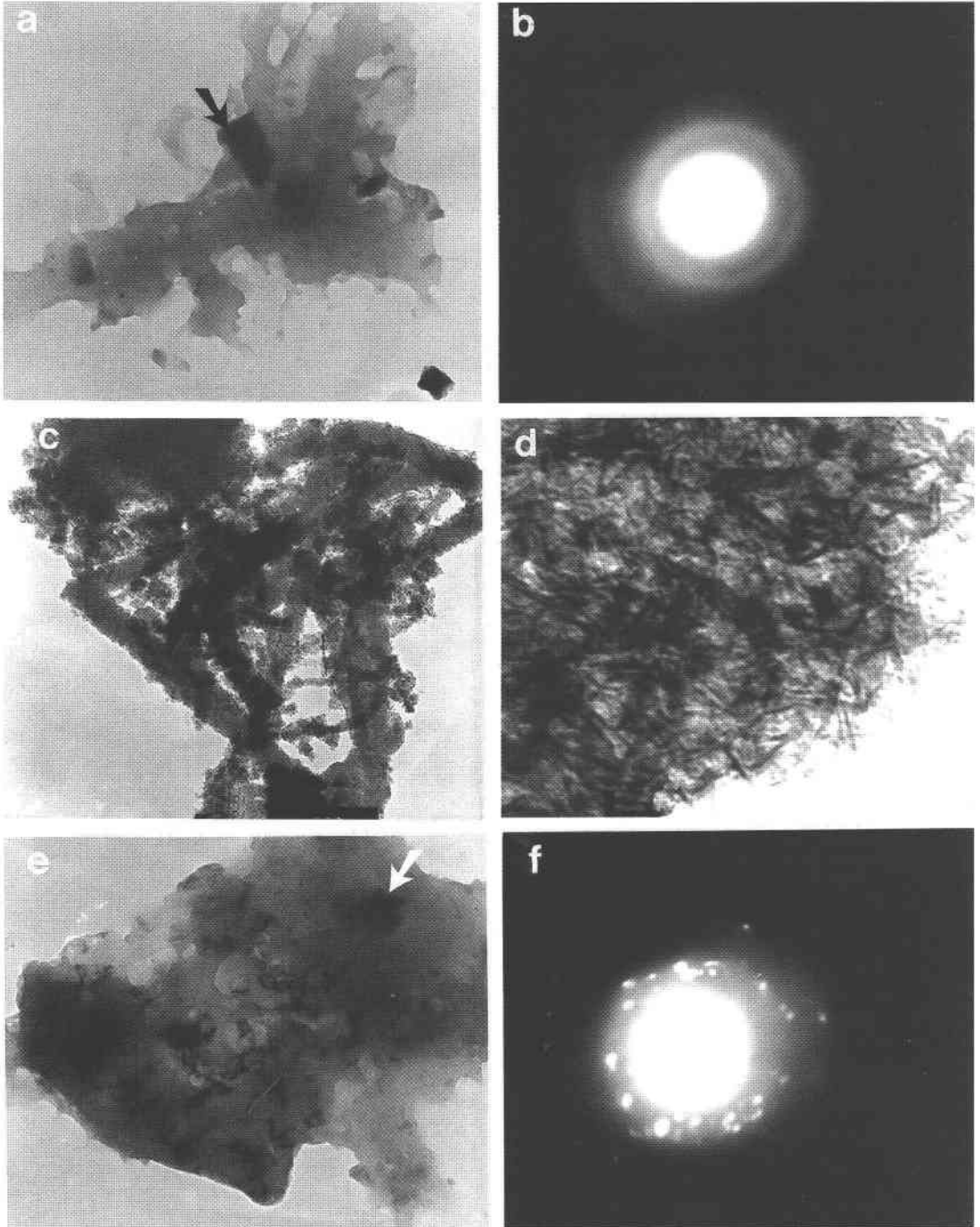
The agglomerates of two-XRD-line ferrihydrite typically are formless masses (Fig. 3a). SAED patterns (Fig. 3b) of these demonstrate the poorly crystalline nature of the material, consistent with the XRD results. The inner bright and outer faint rings are diffuse, in agreement with the initial primitive two-dimensional ordering of the 11 and 30 *hk* planes. High-magnification examination of most of the formless agglomerates shows a granular texture (Fig. 3c, upper left corner); however, some have an elongate lath-like habit (Fig. 3c), whereas others exhibit a filigree form (Fig. 3d). No relationship is observed between composition and these shapes, but those showing distinctive shapes commonly display poorly crystalline SAED patterns similar to that in Figure 3b.

TABLE 3 RESULTS OF EDS ANALYSES OF <2 µm GRAINS OF TWO-XRD-LINE FERRIHYDRITE IN SAMPLE M2192 LOC.1 (106848)

wt. % No.	TEM-1			TEM-2		STEM			Bulk Comp.
	Avg. 10	S.D.	Error	Avg. 11	S.D.	Avg. 28	S.D.	Error	
SiO ₂	21.0	3.6	9	20.2	2.4	25.6	4.2	27	19.7
TiO ₂	b.d.			b.d.		b.d.			0.03
Fe ₂ O ₃	65.2	5.6	8	68.2	5.9	67.7	6.0	32	71.9
Al ₂ O ₃	b.d.			b.d.		b.d.			0.00
MnO	3.4	3.4	20	0.5	0.9	b.d.			3.25
MgO	b.d.			b.d.		b.d.			1.37
CaO	3.0	2.1	17	1.9	1.2	b.d.			1.75
K ₂ O	b.d.			1.1	0.3	b.d.			0.96
Cl ₂ O	3.3	4.2	15	1.1	0.6	b.d.			0.00
P ₂ O ₅	3.0	5.0	17	4.1	3.3	b.d.			4.40
SO ₄	b.d.			2.0	1.8	b.d.			
As ₂ O ₃	b.d.			0.8	0.3	b.d.			0.22
Total	98.9			99.9		93.3			102.7

TEM-1: Department of Material Science, University of Toronto, TEM-2: Geological Survey of Japan (Boyd *et al.* 1993), STEM: Centre for Electron Microscopy, McMaster University. Bulk Composition (Bulk Comp.) is recalculated on a detritus-, volatile- and salt-free bulk composition expressed as oxides (Boyd *et al.* 1993).

No.: number of grains analyzed, b.d.: below limit of detection. The error reported is the theoretical analytical error to two standard deviations (S.D.) based on the net number of counts; it is evaluated by the method used in Williams (1984) and expressed as a percentage of the total amount of the element present. The analytical totals are not necessarily 100% owing to averaging and rejection of data for individual elements whose average contents are calculated to be below the limit of detection based on an analytical error of >=40%. The standard deviation refers to the analytical data obtained.



Agglomerates lacking evidence of contamination have poorly crystalline SAED patterns (Fig. 3b) and are dominated by Fe and Si, with variable minor amounts

of P, S and As (Table 3, Boyd *et al.* 1993). Many have a heterogeneous mottled appearance suggestive of particles that may have been incorporated from the sur-

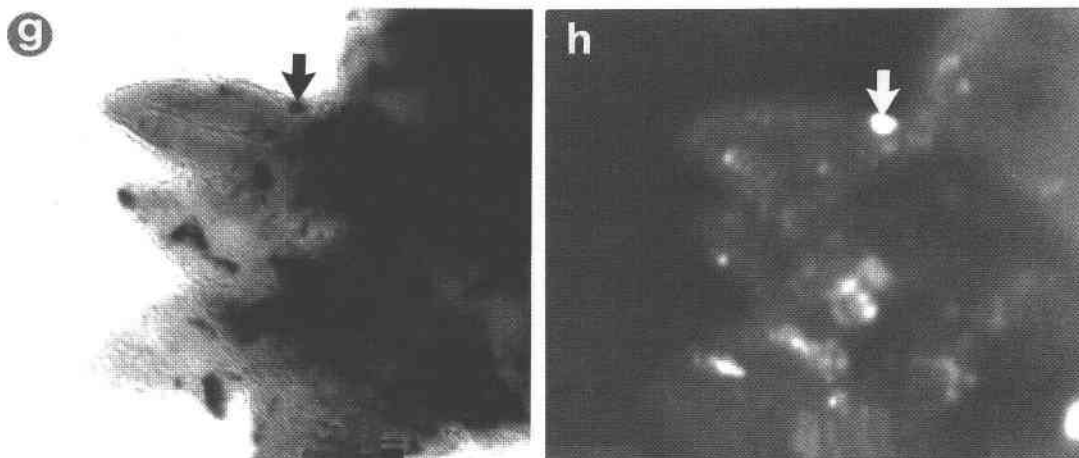


FIG. 3. TEM images of oxyhydroxides at Franklin Seamount. (a) Bright-field image of formless Fe oxyhydroxide (ferrihydrite) agglomerates; darker fragments in the mass are more Fe-rich and are probably filamentous debris (see arrow), sample M2202-2A-1 (106920), height of micrograph 2.6 μm . (b) SAED pattern of material in Figure 3a, showing the poorly crystalline nature of the material. (c) Fe oxyhydroxide agglomerate with lath-like habit, M2192 loc.1 (106848), height of micrograph 1.6 μm . (d) Fe oxyhydroxide agglomerate with filigree texture, M2192 loc.1 (106848), height of micrograph 0.4 μm . (e) Bright-field image of a mixed Fe oxyhydroxide - detritus agglomerate (arrow shows typical fragment), sample M2202-2A-1 (106920), height of micrograph 2.6 μm . (f) SAED pattern of agglomerate in Figure 3e showing the effect of incorporation of the detrital fragments. The spots are too complicated for mineralogical identification. (g) Highly magnified edge of a Fe oxyhydroxide - detritus agglomerate having a non-amorphous SAED pattern (arrow points to incorporated fragment), sample M2202-2A-1 (106920), height of micrograph 0.4 μm . (h) Dark-field image of Figure 3g; the bright specks are highlighted detrital fragments less than 40 nm in size (see arrow). Brightness is caused by centering of the aperture around one of the "non-amorphous" SAED spots such that only the electrons from that source are allowed to pass through; height of micrograph 0.4 μm .

rounding environment (Figs. 3a, e). Such samples exhibit complicated, scattered SAED patterns (Fig. 3f) coincident with significant amounts of K, Mg and Al indicating contamination by mineral and rock fragments. One (Fig. 3g), examined using dark-field imagery by centering the aperture around one of the diffraction points, reveals tiny incorporated submicrometric (<0.04 μm) detrital particles (Fig. 3h).

Some ferrihydrite agglomerates have scattered SAED patterns and significant Ba and S contents, which suggest that they contain tiny fragments of barite from nearby spires in the Franklin Seamount caldera. Others having similar SAED patterns also contain significant amounts of Ca. Fragments of both calcareous and siliceous fossils occur in some samples. The former shows SAED patterns indicative of crystalline matter and contains only Ca, indicating carbonate, whereas the latter is poorly crystalline and contains only Si, indicating opal-A. The presence of incorporated opal-A cannot easily be documented by electron diffraction and is suggested only by the highly variable Si/Fe values.

Results of TEM-EDS spot analyses of particles in the oxyhydroxide samples are plotted in Figures 4 and 5. A broad compositional range exists between the Si-Fe and Fe-Si oxyhydroxides, but even the most Fe-rich

oxyhydroxides contain significant Si. An exception is one grain that displays the acicular prismatic habit of goethite (Cornell *et al.* 1987) and is nearly devoid of Si, in agreement with the electron-microprobe data reported in Binns *et al.* (1993). Figure 4 shows a trend toward the opal-A corner with increased proportions of hydrothermal or fossil silica (or both). Some of the Si-rich particles have submicrometric layers consistent with the presence of carapaces of hydrothermal silica on the Fe-rich filaments. A second trend in Figure 4 is an increase of both Si and Al, compared to the pure Fe oxyhydroxides, toward the spot compositions of discrete detrital fragments in the samples. There is no significant difference in composition between filamentous two-XRD-line ferrihydrite and those non-filamentous agglomerates that lack evidence of opal-A or Si-Al contamination. The presence of separate Si-rich phases is not observed within the more Fe-rich agglomerates, and their Si:Fe ratio is relatively uniform.

Vernadite, birnessite, and nontronite occur in some samples (Fig. 5). This vernadite and that from hydrogenous nodules have a similar Al:Mn ratio (Haynes & Magyar 1987). The paucity of Al and Mg in particles of the Fe-Si smectite (Table 2, Fig. 4) suggests its identification as nontronite. In general, results of the TEM-EDS

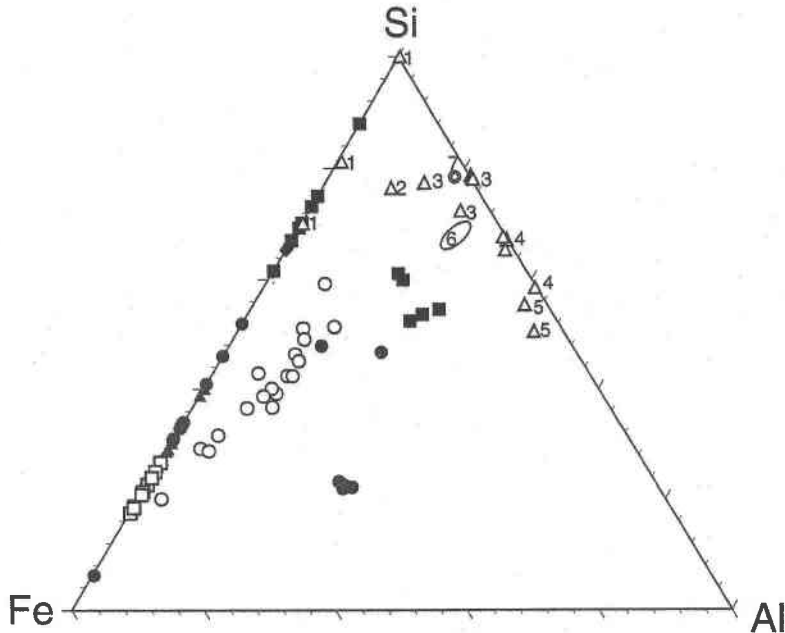


FIG. 4. Fe-Si-Al plot of results of EDS spot analysis of various types of $<2 \mu\text{m}$ agglomerates identified by TEM in oxyhydroxides samples from Franklin Seamount. Filled squares are Si-Fe oxyhydroxides, filled circles are non-filamentous Fe-Si oxyhydroxides, filled triangles are filamentous Fe-Si oxyhydroxides, filled diamonds are nontronite, open squares are birnessite, open circles are vernadite, and open triangles are detrital shards: (1) olivine-serpentine, (2) pyroxene, (3) volcanic glass of rhyolitic to andesitic composition, (4) plagioclase, (5) clay-like or micaceous particles. Silica and carbonate fossil fragments also were identified in samples (not shown). Electron microprobe data for Franklin Seamount andesite (6) and rhyolite (7), taken from Binns *et al.* (1990b) and Binns & Whitford (1987), are shown as an open oval and a double circle.

spot analyses agree well with electron-microprobe analyses on oxyhydroxide minerals given by Binns *et al.* (1993) (Fig. 4) and the bulk compositions given in Table 2. The results demonstrate the credibility of the TEM-EDS approach for spot analysis of micrometric particles that are too small for electron-microprobe analysis.

Traverses of STEM-EDS high-resolution spot analyses were made of two-XRD-line ferrihydrite agglomerates across an elongate lath-like structure (Figs. 6a, b) and into the wall of a filament (Figs. 6c, d). The filament wall has a 20-nm-wide dark zone caused by a Mn-rich layer parallel to the length of the filament wall. Confidence in the spatial resolution of the analyses is supported by the low levels of Mn adjacent to the dark zone. The STEM-EDS analyses of the ferrihydrite indicate a large range in oxygen content, but a relatively constant Si:Fe ratio (Fig. 7). Atomic proportions range from $\text{Fe}_{0.25}\text{Si}_{0.1}\text{O}_{0.65}$ to $\text{Fe}_{0.1}\text{Si}_{0.05}\text{O}_{0.85}$. These proportions agree with the bulk compositions of the sample plotted in Table 2 if the LOI component is assumed to

comprise equal amounts of H_2O and OH. If the Si is not structurally incorporated into the ferrihydrite but instead is sorbed on its surface, the composition ranges then from $\text{Fe}_{0.28}\text{O}_{0.72}$ to $\text{Fe}_{0.11}\text{O}_{0.89}$.

High magnification of the STEM system facilitates imaging of the individual crystallites of ferrihydrite. Figure 6e shows the presence of numerous randomly stacked crystallites and bubble-like spheres, 2 to 9 nm in diameter. Only a few layers of the crystallites are needed to mask any indication of order or structure in the agglomerate. The crystallites appear to have denser edges 1–2 nm in width compared to their cores. Spot analyses of individual edges and cores of crystallites lack major-element peaks, reflecting their extreme thinness perpendicular to the plane of the image. The XRD evidence for an absence of order in the third dimension is consistent with the crystallites, being very thin. This attribute, combined with the randomly stacked nature of agglomerated crystallites suggest that the crystallites have a platy granular habit like that of natural two-XRD-line ferrihydrite from surface springs (Eggleton 1987).

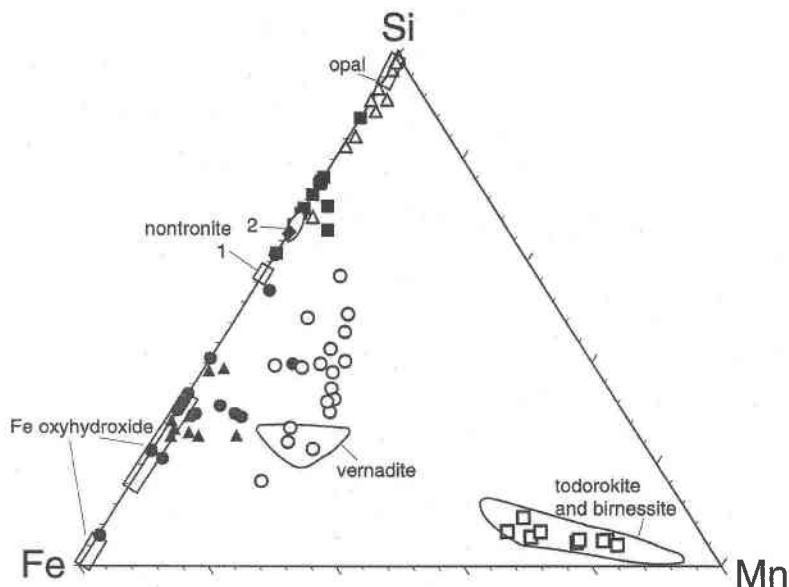


FIG. 5. Fe-Si-Mn plot of results of EDS spot analysis of various types of $<2 \mu\text{m}$ agglomerates identified by TEM in oxyhydroxides samples from Franklin Seamount. Filled squares are Si-Fe oxyhydroxides, filled circles are non-filamentous Fe-Si oxyhydroxides, filled triangles are filamentous Fe-Si oxyhydroxides, filled diamonds are nontronite, open squares are birnessite, open circles are vernadite, and open triangles are detrital shards. The outlined areas represent compositions of constituent phases from the electron-microprobe data of Binns *et al.* (1993), except for nontronite (2), which is from the composition reported in Chamley (1989). The position of the Si-free composition near the Fe corner is probably due to goethite. Other Fe oxyhydroxides are ferrihydrite. The Si-Fe oxyhydroxides are mixtures of ferrihydrite, opal-A, and detritus.

On the basis of the STEM images, the specific surface-area of individual two-XRD-line ferrihydrite crystallites has been estimated from their diameter using basic geometrical relationships (McCrone 1973) and an average density for ferrihydrite of 3.96 g/cm^3 (Schwertmann & Cornell 1991). Crystallites 2 to 9 nm in diameter have specific surface-areas that range approximately from 1400 to $300 \text{ m}^2/\text{g}$, modeled as circular plates with dimensions of 1 : 1 : 0.1. For comparison, Eggleton & Fitzpatrick (1988) calculated a range of higher specific surface-areas, 1900 to $550 \text{ m}^2/\text{g}$ for diameters of 2.6 to 5.0 nm and densities of 3.2 to 3.8 g/cm^3 , for truncated hexagonal bipyramidal crystals of the more ordered six-line variety of ferrihydrite.

DISCUSSION

Deposits of poorly crystalline Fe oxyhydroxides similar to those at Franklin Seamount have been described as hydrothermal crusts and mounds from Lau and North Fiji basins (von Stackelberg *et al.* 1990), south Pacific hot spots (Hekinian *et al.* 1993, Stoffers *et al.* 1993), Loihi Seamount (Cremer 1994, DeCarlo *et al.* 1983), 11–13°N East Pacific Rise (Hekinian *et al.*

1993, Alt 1988), and the Mid-Atlantic Ridge (Herzig *et al.* 1991, Hannington *et al.* 1988). The rarity at Franklin Seamount of crystalline Fe oxides such as hematite and goethite is a significant difference, but is consistent with the expected mineralogy of fresh precipitates from actively venting chimneys. Ferrihydrite is thermodynamically unstable relative to goethite or hematite, so will eventually transform to those minerals (Murray 1979).

Iron-rich samples from ancient hydrothermal mounds or crusts on the seafloor, such as on Cretaceous seamounts in the central Pacific (Hein *et al.* 1994), are dominated by goethite. In contrast, Stoffers *et al.* (1993) and Boyd *et al.* (1993) described poorly crystalline Fe oxyhydroxide as the major phase in samples from the Teahitia Seamount, where actively venting chimneys occur (Hekinian *et al.* 1993). Hydrothermal two-XRD-line ferrihydrite has been identified from seafloor sites by Stoffers *et al.* (1993); other investigators have referred to such material as poorly crystalline Fe oxide, Fe oxyhydroxide, ferric Fe gel, protoferrihydrite and, in some cases, erroneously as goethite.

The hydrothermal origin of birnessite and nontronite at Franklin Seamount is indicated by their presence in samples from actively venting chimneys. Manganese

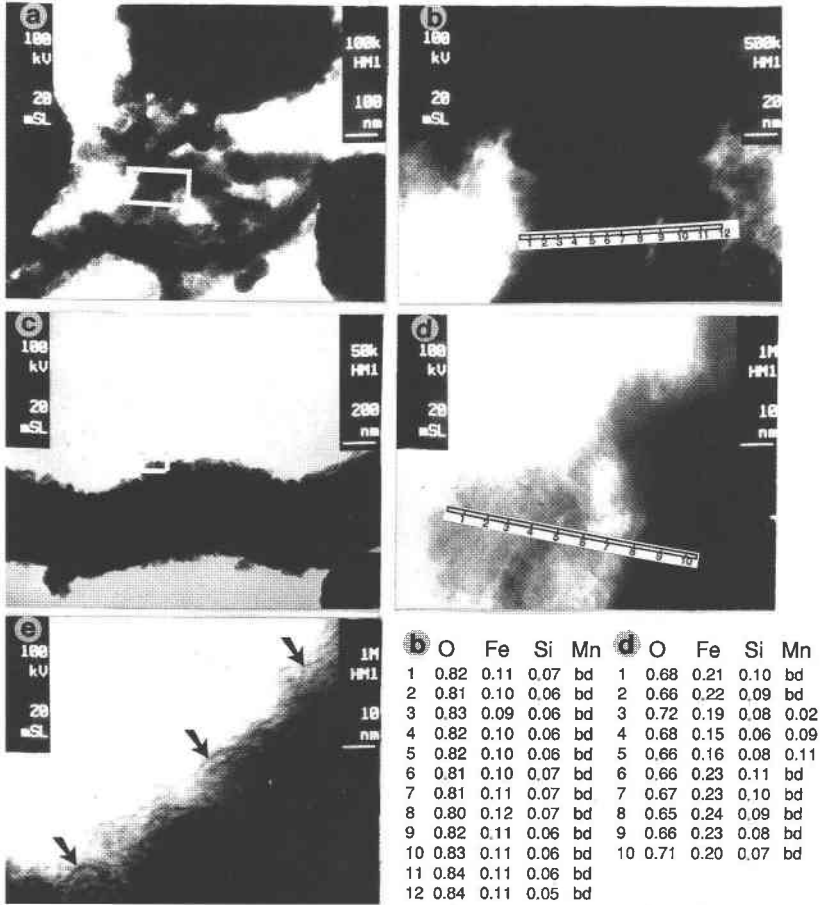


FIG. 6. High-magnification STEM images of ferrihydrite agglomerates, sample M2192 loc.1 (106848). (a) Lath-like ferrihydrite; box represents area of Figure 6b. (b) Close-up showing atomic proportion (EDS data) along a traverse across the lath in Figure 6a (1-12). (c) Filament; box represents area of Figure 6d. (d) Close-up showing atomic proportion (EDS data) along a traverse across the edge of a filament in Figure 6c (1-10). The spot caused by beam damage directly beside the number 5 in 6d indicates the spatial resolution of the EDS analyses. (e) Close-up of ferrihydrite agglomerate showing a bubble-like structure of individual crystallites (see arrows). The diameter of the crystallites is highly variable and ranges from 2 to 9 nm. The level of Mn is in some cases below detection (bd).

minerals in these samples tend to be confined to separate layers, suggestive of accumulation during lulls in venting activity. However, the relatively high manganese content of 0.01 mM/kg in a sample of vent fluid (Binns *et al.* 1993) and preservation in some instances of submicroscopic Mn-rich zones in the ferrihydrite aggregates (Fig. 6d) suggest that some of the manganese precipitated with the iron.

Lisitsin *et al.* (1991) proposed that the abundant nontronite in the cores of many chimney samples at

Franklin Seamount is explained by the diagenetic reduction of the Si-rich poorly crystalline Fe oxyhydroxides. Binns (1990) observed light green ferrous trioctahedral smectite, similar in appearance to the reduced precursor to nontronite described in Decarreau & Bonnin (1986), occurring on the surface of an actively venting chimney close to the vent orifice. This is consistent with the direct precipitation of at least a portion of the smectite from the venting hydrothermal fluids. Hannington (1986) reported voluminous nontronite on

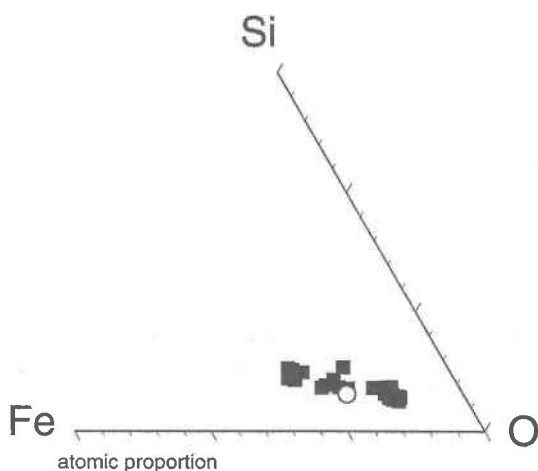


FIG. 7. Truncated Fe-Si-O diagram showing results of high-resolution STEM-EDS spot analyses of ferrihydrite in sample M2192 loc.1 (106848). Squares represent results of EDS spot analyses; open circle is the bulk composition of the sample. Oxygen content for bulk analyses is calculated from the oxide content of the major elements for which the LOI (loss on ignition) is assumed to be half H_2O and half OH.

the seafloor among the sulfide-sulfate spires of Axial Seamount in the northeastern Pacific.

Hydrothermal oxyhydroxides are commonly located on the margins of sulfide or sulfate occurrences, such as at Franklin Seamount (Boyd *et al.* 1993, Binns *et al.* 1993), $12^{\circ}43'\text{N}$, East Pacific Rise (Hekinian *et al.* 1993, Boyd *et al.* 1993), Explorer Ridge, (Scott *et al.* 1990, Tunncliffe *et al.* 1986), southern Lau Basin (von Stackelberg *et al.* 1990) and the Mid-Atlantic Ridge (Herzig *et al.* 1991, Hannington *et al.* 1988). Many other deposits of Fe oxyhydroxide, however, lack spatial associations with sulfur-bearing mounds and chimneys, such as on the central Pacific seamounts (Hein *et al.* 1994), $11^{\circ}30'\text{N}$, East Pacific Rise (Hekinian *et al.* 1993, Boyd *et al.* 1993), South Pacific hotspots (Stoffers *et al.* 1993, Hekinian *et al.* 1993, Boyd *et al.* 1993), and Loihi Seamount (Cremer 1994, DeCarlo *et al.* 1983). These solitary deposits seem to occur preferentially, but not exclusively, on intraplate seamounts.

The poorly crystalline Fe oxyhydroxide at Franklin Seamount is similar to the primitive two-XRD-line ferrihydrite described in surface environments in contact with the atmosphere, such as acid mine-drainage (Bigham *et al.* 1992, Ferris *et al.* 1989), ferriiferous groundwater springs (Childs *et al.* 1982, Carlson & Schwertmann 1981), lake sediments (Fortin *et al.* 1993) and soils (Lindsay 1979). In addition, primitive Fe oxides (probably ferrihydrite) typically occurs in hydrogenous crusts and nodules on the deep seafloor (Murray

1979) and is reported to cover bacterial surfaces at southern Explorer Ridge, northeast Pacific Ocean (Fortin *et al.* 1998). Its formation is limited to conditions where Fe^{2+} is oxidized rapidly and where inhibitors of crystallization such as silica, phosphate, and organic materials are present (Schwertmann & Cornell 1991). At Franklin Seamount, the ferrihydrite forms in an environment in which reduced, acidic, Fe-rich, vent fluids carrying Si and P (Binns *et al.* 1993) mix rapidly with slightly alkaline, oxidized seawater. The high contents of Si and P in the ferrihydrite record this environment of precipitation, and its preservation in inactive mounds and chimneys is aided by these inhibitors of crystallization. The highly siliceous nature of the ferrihydrite at Franklin Seamount reflects the high Si:Fe ratio, 8.7, measured in a sample of vent fluid collected from an active chimney during the same expedition in which the rock samples were collected (Binns *et al.* 1993). Those ferrihydrite aggregates that exhibit a granular morphology commonly contain major amounts of Si. Carlson & Schwertmann (1981) and Ferris *et al.* (1989) found similar morphologies in natural Si-rich ferrihydrite from surface environments.

The two-XRD-line ferrihydrite samples from Franklin Seamount are characterized by high Si contents, relatively constant Si/Fe values, and a distinctive XRD hump at a higher d -value than that of the Si-free material. These characteristics, combined with stability under the TEM electron beam and its persistence to 570°C , suggest that the Si is very strongly bonded to the crystallites and may be contained in the atomic structure of the mineral. These results serve as the basis for a proposed compositional model for two-XRD-line ferrihydrite.

COMPOSITIONAL MODEL FOR FERRIHYDRITE

The chemical formula for ferrihydrite has not been fully established because of the large variability in its composition and atomic structure, particularly in the coordination of the Fe. Specifically, (1) the composition of ferrihydrite is variable because crystallinity of the material varies from a primitive two-dimensional two-XRD-line type to the better-crystallized three-dimensional six-XRD-line mineral, and (2) the formula for synthetic ferrihydrite does not necessarily match that of its natural equivalent. The latter situation arises because of the great diversity of physical environments in which ferrihydrite forms. Previously proposed chemical formulas based primarily on synthetic ferrihydrite are summarized in Table 4.

The study of hydrothermal two-XRD-line ferrihydrite from Franklin Seamount provides for a better understanding of the composition of natural ferrihydrite. Previous investigators have suggested that the Si in ferrihydrite is sorbed on its surface from the surrounding aqueous solution, probably as the anion HSiO_4^{3-} . Figure 8, based on STEM-EDS and TEM-EDS spot

TABLE 4. COMPOSITIONS OF FERRIHYDRITE PROPOSED IN THE LITERATURE

Fe(OH) ₃	Ferric iron hydroxide gel before hydration to ferrihydrite. Thermodynamic data for Fe(OH) ₃ and ferrihydrite commonly quoted interchangeably (Schwertmann & Cornell 1991, Lindsay 1979).
FeO(OH)	Van der Giessen (1966)
5Fe ₂ O ₃ ·9H ₂ O	Schwertmann & Cornell (1991)
Fe ₃ HO ₈ ·4H ₂ O	Towe & Bradley (1967)
Fe ₃ (O,H) ₃	Chukhrov <i>et al.</i> (1973)
Fe ₂ O ₃ ± 2FeOOH·2.6H ₂ O	Russell (1979)
Fe ₄ (O,OH,H ₂ O) ₁₂	Two-XRD-line ferrihydrite, Eggleton & Fitzpatrick (1988)
Fe _{4.6} (O,OH,H ₂ O) ₁₂	Six-XRD-line ferrihydrite, Eggleton & Fitzpatrick (1988)
Fe _{4.6} Si _{1.07} O _{6.08} (OH) _{3.92}	50 Å ferrihydrite crystallite with adsorbed silica (see text), Eggleton & Fitzpatrick (1988)
^{VI} Fe _{2.9} ^{IV} (Si,Fe,Al) _{1.3} (O,OH,H ₂ O) ₁₂	Two-XRD-line ferrihydrite, this study

analyses of ferrihydrite crystallites and aggregates (M2192 loc.1 106848), shows the relationship between the Si and Fe. Much of the Si may have been incorporated into the ferrihydrite structure rather than sorbed on the surface because the Fe:Si ratio remains relatively constant despite the variable spatial resolution of the analyses. Eggleton & Fitzpatrick (1988) proposed, in their structural model of ferrihydrite, that 35% of the Fe is in tetrahedral coordination. They suggested further that Si replacing Fe in the tetrahedral sites might be expected to make the mineral more stable thermally because it would block transformation to hematite, in which all the Fe is octahedrally coordinated. The dark line in Figure 8 labeled 35% Si is the expected Si:Fe ratio in ferrihydrite if Si occupies all of the tetrahedral sites. This line provides a reasonably good fit to the data, compared to the fainter line derived from the least-squares regression for the analytical data.

Fortin *et al.* (1993) found Fe oxyhydroxides from lake sediments, which are dominated by two-XRD-line ferrihydrite, with Si/Fe values that approximate those found in this study. They are, however, three to five orders of magnitude greater than that calculated from the two-layer surface-complexation model of Dzomback & Morel (1990) for adsorption by ferrihydrite [as shown by the area labeled "sorbed Si (2)" in Fig. 8]. Fortin *et al.* (1993) therefore concluded that sorption of Si alone cannot explain the measured Si/Fe values. In contrast, the analyzed and calculated ratios SO₄/Fe and PO₄/Fe assuming adsorption, although highly variable, fall in the range of the ferrihydrite data from the Franklin Seamount.

Infrared spectroscopic analyses of ferrihydrite shows broad band at 930 cm⁻¹ indicative of Si–O stretching of Si–O–Fe bonds (Carlson & Schwertmann 1981). This inference implies that the Si is an essential component of the ferrihydrite structure rather than merely being bonded to surface oxygen atoms or OH ligands, although Cornell *et al.* (1987) suggested that such linkages can exist both on the surface of and within the ferrihydrite. Normalized X-ray absorption pre-edge spectra (XANES) of natural two- and six-XRD-line ferrihydrites provide evidence for the absence of tetrahedrally coordinated Fe³⁺ (Manceau *et al.* 1990). Both the intensity and structure of the ferrihydrite spectra are close to those of goethite, for which all the Fe is octahedrally coordinated, and these spectra are distinct from those of maghemite, which has 30% tetrahedrally coordinated Fe. The ferrihydrite used in the Manceau *et al.*

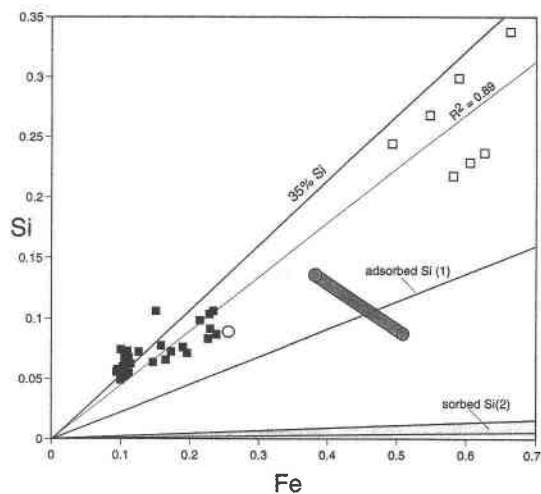


Fig. 8. Atomic proportions of Fe *versus* Si for STEM-EDS (closed squares) and TEM-EDS analyses (open squares) of different agglomerates of ferrihydrite in sample M2192 loc.1 (106848). Bulk analysis of the sample is shown as the open circle. Thin line is the least-squares regression of the points forced through the origin. Upper line corresponds to the Fe:Si ratio in the case where Si replaces all of the Fe in tetrahedrally coordinated sites based on a proposal by Eggleton & Fitzpatrick (1988) that 35% of the Fe is tetrahedrally coordinated. Line labeled "adsorbed Si (1)" represents the Fe:Si ratio for adsorbed Si in the proportion of three surface oxygen atoms with one OH completing a surface tetrahedron, as calculated by Eggleton & Fitzpatrick (1988). Lightly shaded area labeled "sorbed Si (2)" represents the expected Fe:Si ratio for sorbed Si from surface thermodynamic calculations on lacustrine diagenetic ferrihydrite by Fortin *et al.* (1993) using a model proposed by Dzomback & Morel (1990). Dark shaded bar shows the range of Si/Fe values for ferrihydrite of 50 Å particle size from surface springs (Childs *et al.* 1982).

(1990) study, however, is Si-rich, and was obtained from samples used in the Carlson & Schwertmann (1981) study. Si has too low an atomic number to be identified by XANES if it has replaced Fe in tetrahedrally coordinated sites.

Combes *et al.* (1990) found no evidence in X-ray absorption spectra for the presence of tetrahedrally coordinated Fe in a synthesized transient phase formed during the transformation of a ferric gel to hematite. The XRD pattern of this transient phase is similar to that of two-XRD-line ferrihydrite, but when this material was stored in water at 92°C, it lasted only 1–6 hours before crystallizing to hematite. These results, rather than refuting the Eggleton and Fitzpatrick model for the presence of tetrahedrally coordinated Fe, suggest that tetrahedrally coordinated cations, whether they be Fe, Si, or Al, are necessary to stabilize the structure of ferrihydrite.

Zhao *et al.* (1994) found that X-ray absorption fine structure (XAFS) spectra of ferrihydrite record the presence of sites of lower than octahedral, and probably tetrahedral, coordination. They suggested that the atomic structure of ferrihydrite is different on its surface than in its core. These sites of lower coordination would be occupied by Fe, Si or Al on the surface, and this surface configuration of atoms would dominate the structure of two-XRD-line ferrihydrite if the crystallites were thin enough to lack atomic order in a third dimension. As the crystallites amalgamated to form the more evolved six-XRD-line ferrihydrite with three-dimensional *hkl* ordering, these surface cations would become an integral part of the core of the crystal. Manceau & Gates (1997) studied the spectral results of Zhao *et al.* and interpreted the differences in the atomic structure from the surface to the core as a function of the modification of the geometry of the surface iron due to contact with water. They could not rule out, however, the presence of significant amounts of tetrahedrally coordinated iron. In their review, Jambor & Dutrizac (1998) stated that the role of iron in the structure is still uncertain, and likely to be the subject of continued debate.

From low-angle XRD measurements, Parfitt *et al.* (1992) proposed that primary particles of two-XRD-line ferrihydrite 25 Å in diameter consist of crystalline Fe–Si–O domains 7.7 Å across in the *x–y* plane. The size of these domains is comparable to that of the hexagonal unit-cell for six-line ferrihydrite, *a* 5.08, *c* 9.4 Å, as proposed by Towe & Bradley (1967). On the basis of the analyses in this study, the suggested range in composition of two-XRD-line ferrihydrite from the Franklin Seamount is Fe_{0.25}Si_{0.11}(O,OH,H₂O)_{0.64} to Fe_{0.12}Si_{0.05}(O,OH,H₂O)_{0.83}, with an average of Fe_{0.18}Si_{0.08}(O,OH,H₂O)_{0.75}. A more general average composition based on 12(O + OH + H₂O) is (Fe)_{2.9}(Si,Fe,Al)_{1.3}(O,OH,H₂O)₁₂ (Table 4) is proposed for the samples. The Si/Fe values obtained from the STEM–EDS, TEM–EDS and bulk analysis are nearly twice that of the composition Fe_{4.6}Si_{1.07}O_{6.08}(OH)_{5.92} calculated by Eggleton

& Fitzpatrick (1988), if Si is adsorbed in the proportion of one Si to three surface atoms of oxygen, with OH completing a surface tetrahedron in a 50 Å polyhedron (Fig. 8).

In summary, both the structure and composition of natural and synthetic two-XRD-line ferrihydrite are variable, depending on its crystal size. Its composition is also dependent on its mode of formation. Caution thus is advised in assuming that the atomic structures and thus formulas derived for synthetic ferrihydrite can be used to describe natural analogs.

CONCLUSIONS

Bulk and EDS chemical analyses and XRD confirm that the hydrothermal oxyhydroxide deposits at Franklin Seamount are dominated by two-XRD-line ferrihydrite. Nontronite and birnessite are major hydrothermal minerals in the deposits, whereas opal-A is less common and occurs as a major constituent in only a few samples, in which it forms a carapace on agglomerates of ferrihydrite.

Hydrothermal two-XRD-line ferrihydrite from Franklin Seamount is characterized by both high Si contents and relatively constant Si/Fe values in comparison to the Fe/O and Si/O values. The high Si contents are not accounted for by sorption of silica onto the 2–9 nm diameter crystallites of ferrihydrite. Silicon instead appears to have been incorporated into the atomic structure of the mineral, probably replacing Fe in tetrahedral sites. This interpretation is supported by thermal stability of the ferrihydrite up to 570°C, and by its XRD pattern that shows a shift in the broad hump from 2.5 Å to higher *d*-values with increases in Si content. The Si is inferred to provide stability to the structure of ferrihydrite, thus allowing it to persist over a wide range in temperature. On the basis of these findings, an average composition for the two-XRD-line ferrihydrite at Franklin Seamount is suggested to be ^{VI}(Fe)_{2.9}^{IV}(Si, Fe, Al)_{1.3}(O,OH,H₂O)₁₂.

ACKNOWLEDGEMENTS

Samples analyzed by INAA were irradiated at the University of Toronto low-flux Slowpoke Nuclear Reactor under the supervision of Ron Hancock and Susan Aufreiter, and counted in the Department of Geology with the aid of Michael Gorton. Serbie Petrov of the Department of Chemistry, University of Toronto, and David Crabtree of the Ontario Geological Survey, Sudbury, aided in XRD analysis of the samples. Katsumi Marumo of the Geological Survey of Japan, Geoff Whitehead of the Department of Metallurgy and Materials Science, University of Toronto, and Fred Pearson of McMaster University, Hamilton, are thanked for their guidance in electron microscopy. Bob Ramik of the Royal Ontario Museum completed the TGA–DTA analyses and, together with Fred Wicks, provided

advice on ferrihydrite nomenclature. Claudio Cernignani of the Department of Geology, University of Toronto provided the microprobe standards. The Walker Mineralogical Club is thanked for the encouragement and financial support to Boyd, which aided in completing this research. The authors thank Enver Murad and an anonymous referee for their incisive comments, which helped us focus this manuscript. The research was completed in cooperation with IGCP Project #318: Genesis and Correlation of Marine Polymetallic Oxides and supported by grants to Scott from the Natural Sciences and Engineering Research Council of Canada and The Bank of Nova Scotia.

REFERENCES

- ALT, J.C. (1988): Hydrothermal oxide and nontronite deposits on seamounts in the eastern Pacific. *Mar. Geol.* **81**, 227-239.
- BARNES, S. & GORTON, M.P. (1984): Trace element analysis by neutron activation with a low flux reactor (Slowpoke-II): results for international reference rocks. *Geostandards Newsletter* **8**, 17-23.
- BENES, V., SCOTT, S.D. & BINNS, R.A. (1994): Tectonics of rift propagation into a continental margin: western Woodlark Basin, Papua New Guinea. *J. Geophys. Res.* **99**, 4439-4455.
- BIGHAM, J. M., SCHWERTMANN, U. & CARLSON, L. (1992): Mineralogy of precipitates formed by the biogeochemical oxidation of Fe(II) in mine drainage. In *Biomineralization Processes of Iron and Manganese Modern and Ancient Environments* (H.C.W. Skinner & R.W. Fitzpatrick, eds.). *Catena, Suppl.* **21**, 219-232.
- BINNS, R.A. (1990): Report on SUPACLARK Dive 7 on Mir-2 submersible: Franklin Seamount, Woodlark Basin PNG. *CSIRO Division of Exploration Geoscience, Restricted Rep.* **140R**.
- _____, SCOTT, S.D., BOGDANOV, Y.A., LISITSIN, A.P., GORDEEV, V.V., GURVICH, E.G., FINLAYSON, E.J., BOYD, T., DOTTER, L.E., WHELLER, G.E. & MURAVYEV, K.G. (1993): Hydrothermal oxide and gold-rich sulfate deposits of Franklin Seamount, western Woodlark basin, Papua New Guinea. *Econ. Geol.* **88**, 2122-2153.
- _____, _____, WHELLER, G.E. & BENES, V. (1990a): Report on the SUPACLARK cruise, Woodlark Basin, PNG, April 8-18 1990, RV Akademik Mstislav Keldysh. *CSIRO Division of Exploration Geoscience, Open File* **176R**.
- _____, WHELLER, G.E. & GOULD, K.W. (1990b): Electron microprobe survey of glass compositions in mafic volcanic rocks collected during the 1990 SUPACLARK cruise from the western Woodlark Basin, Papua New Guinea. *CSIRO Division of Exploration Geoscience, Restricted Rep.* **181R**.
- _____ & WHITFORD, D.J. (1987): Volcanic rocks from the western Woodlark Basin, Papua New Guinea. *Pacific Rim Congress '87*.
- BOGDANOV, YU.A., LISITSIN, A.P., BINNS, R.A., GORSHKOV, A.I., GURVICH, E.G., DRITZ, V.A., DUBININA, G.A., BOGDANOVA, O.YU, SIVKOV, A.V. & KUPTSOV, V.M. (1997): Low-temperature hydrothermal deposits of Franklin Seamount, Woodlark Basin, Papua New Guinea. *Mar. Geol.* **142**, 99-117.
- BOYD, T. (1996): *The Geochemistry and Mineralogy of a Hydrothermal Oxyhydroxide Deposit at Franklin Seamount, Western Woodlark Basin, Papua New Guinea*. Ph.D. thesis, Univ. Toronto, Toronto, Ontario.
- _____, SCOTT, S.D. & HEKINIAN, R. (1993): Trace element patterns in Fe-Si-Mn oxyhydroxides at three hydrothermally active seafloor regions. *Resour. Geol., Spec. Issue* **17**, 83-95.
- CAMPBELL, A.S., SCHWERTMANN, U. & CAMPBELL, P.A. (1997): Formation of cubic phases on heating ferrihydrite. *Clay Minerals* **32**, 615-622.
- CARLSON, L. & SCHWERTMANN, U. (1981): Natural ferrihydrites in surface deposits from Finland and their association with silica. *Geochim. Cosmochim. Acta* **45**, 421-429.
- CHAMLEY, H. (1989): *Clay Sedimentology*. Springer-Verlag, Berlin, Germany.
- CHILDS, C.W., DOWNES, C.J. & WELLS, N. (1982): Hydrous iron oxyhydroxide minerals with short range order deposited in a spring/stream system, Tongariro National Park, New Zealand. *Aust. J. Soil. Res.* **20**, 119-129.
- CHUKHROV, F.W., ZVYAGIN, B.B., YERMILOVA, L.P. & GORSHOV, A.I. (1973): New data on Fe-silica oxyhydroxides in the weathering zone. In *Proc. Int. Clay Conf. (Madrid, 1970)* (J.M. Serratos, ed.), Div. de Ciencias, C.S.I.C., Madrid, Spain (333-341).
- _____, _____ & _____ (1976): Mineralogical criteria in the origin of marine iron-manganese nodules. *Mineral. Deposita* **11**, 24-32.
- CLIFF, G. & LORIMER, G.W. (1975): The quantitative analysis of thin specimens. *J. Microscopy* **103**, 203-207.
- COMBES, J.M., MANCEAU, A. & CALAS, G. (1990): Formation of ferric oxides from aqueous solutions: a polyhedral approach by X-ray absorption spectroscopy. II. Hematite formation from ferric gels. *Geochim. Cosmochim. Acta* **54**, 1083-1091.
- CORNELL, R.M., GIOVANOLI, R. & SCHINDLER, P.W. (1987): Effect of silicate species on the transformation of ferrihydrite into goethite and hematite in alkaline media. *Clays Clay Minerals* **35**, 21-28.
- CREMER, M.D. (1994): *Geochemistry of Hydrothermal Deposits from the Summit Region of Loihi Seamount, Hawaii*. M.Sc. thesis, Univ. Hawaii, Honolulu, Hawaii.
- DE CARLO, E.H., MCMURTRY, G.M. & YEH, HSUEH-WEN (1983): Geochemistry of hydrothermal deposits from Loihi submarine volcano, Hawaii. *Earth Planet. Sci. Lett.* **66**, 438-449.

- DECARREAU, A. & BONNIN, D. (1986): Synthesis and crystallogenesis at low temperature of Fe(III)- smectites by evolution of coprecipitated gels: experiments in partially reducing conditions. *Clay Minerals* **21**, 861-877.
- DZOMBAK, D.A. & MOREL, F.M. (1990): *Surface Complexation Modeling of Hydrous Ferric Oxide*. John Wiley & Sons, New York, N.Y.
- EGGLETON, R.A. (1987): Noncrystalline Fe-Si-Al-oxyhydroxides. *Clays Clay Minerals* **35**, 29-37.
- _____ & FITZPATRICK, R.W. (1988): New data and a revised structural model for ferrihydrite. *Clays Clay Minerals* **36**, 111-124.
- FERRIS, F.G., TAZAKI, K. & FYFE, W.S. (1989): Iron oxides in acid mine drainage environments and their association with bacteria. *Chem. Geol.* **74**, 321-330.
- FORTIN, D., FERRIS, F.G. & SCOTT, S.D. (1998): Formation of Fe-silicates and Fe-oxides on bacterial surfaces in samples collected near hydrothermal vents on the Southern Explorer Ridge in the northeast Pacific Ocean. *Am. Mineral.* **83**, 1399-1408.
- _____, LEPPARD, G.G. & TESSIER, A. (1993): Characteristics of lacustrine diagenetic iron oxyhydroxides. *Geochim. Cosmochim. Acta* **57**, 4391-4404.
- GIOVANOLI, R. & ARRHENIUS, G. (1988): Structural chemistry of marine manganese and Fe minerals and synthetic model compounds. In *The Manganese Nodule Belt of the Pacific Ocean, Geological Environment, Nodule Formation and Mining Aspects* (P. Halbach, G. Friedrich & U. von Stackelberg, eds.). Ferdinand Enke Verlag, Stuttgart, Germany (20-37).
- GODDARD, E.N., TRASK, P.D., DE FORD, R.K., ROVE, O.N., SINGEWALD, J. JR. & OVERBECK, R.M. (1948): *Rock Color Chart*. The Rock-Color Chart Committee, Geological Society of America, Boulder, Colorado.
- HANNINGTON, M.D. (1986): *Geology, Mineralogy and Geochemistry of a Silica - Sulphate - Sulphide Deposit, Axial Seamount, N.E. Pacific Ocean*. M.Sc. thesis, Univ. Toronto, Toronto, Ontario.
- _____, THOMPSON, G., RONA, P.A. & SCOTT, S.D. (1988): Gold and native copper in supergene sulphides from the Mid-Atlantic Ridge. *Nature* **333**, 64-66.
- HAYNES, B.W. & MAGYAR, M.J. (1987): Analysis and metallurgy of manganese nodules. In *Marine Minerals* (P.G. Teleki, M.R. Dobson, J.R. Moore & U. von Stackelberg, eds.). Advances in Research and Resource Assessment, NATO Advanced Study Research Institute **194**, 235-247.
- HEIN, J.R., YEH, HSUEH-WEN, GUNN, S.H., GIBBS, A.E. & WANG, CHUNG-HO (1994): Composition and origin of hydrothermal ironstones from central Pacific seamounts. *Geochim. Cosmochim. Acta* **58**, 179-189.
- HEKINIEN, R., HOFFERT, M., LARQUÉ, P., CHEMINÉE, J.L., STOFFERS, P. & BIDEAU, D. (1993): Hydrothermal Fe and Si oxyhydroxide deposits from South Pacific intraplate volcanoes and the East Pacific Rise axial and off-axial regions. *Econ. Geol.* **88**, 2099-2121.
- HERZIG, P.M., HANNINGTON, M.D., SCOTT, S.D., MALIOTIS, G., RONA, P.A. & THOMPSON, G. (1991): Gold-rich seafloor gossans in the Troodos ophiolite and on the Mid-Atlantic Ridge. *Econ. Geol.* **86**, 1747-1755.
- JAMBOR, J.L. & DUTRIZAC, J.E. (1998): Occurrence and constitution of natural and synthetic ferrihydrite, a widespread iron oxyhydroxide. *Chem. Rev.* **98**, 2549-2585.
- JONES, J.B. & SEGNIIT, E.R. (1971): The nature of opal. 1. Nomenclature and constituent phases. *Geol. Soc. Aust.* **18**, 57-68.
- JUNIPER, S.K. & FOUQUET, Y. (1988): Filamentous iron-silica deposits from modern and ancient hydrothermal sites. *Can. Mineral.* **26**, 859-869.
- LINDSAY, W.L. (1979): *Chemical Equilibria in Soils*. John Wiley & Sons, New York, N.Y.
- LISITSIN, A., BINNS, R.A., BOGDANOV, YU.A., SCOTT, S.D., ZONENSHAYN, L.P., GORDEYEV, V.V., GURVICH, YE.G., MURAV'YEV, K.G. & SEROVA, V.V. (1991): Active hydrothermal activity at Franklin Seamount, western Woodlark Sea (Papua New Guinea). *Int. Geol. Rev.* **33**, 914-929.
- MACKENZIE, R.C. & BERGGREN, G. (1970): Oxides and hydroxides of higher valence elements. In *Differential Thermal Analysis I* (R.C. Mackenzie, ed.). Academic Press, New York, N.Y. (272-302).
- MANCEAU, A., COMBES, J.-M. & CALAS, G. (1990): New data and a revised structural model for ferrihydrite: comment. *Clays Clay Minerals* **38**, 331-334.
- _____ & GATES, W.P. (1997): Surface structural model for ferrihydrite. *Clays Clay Minerals* **45**, 448-460.
- MCCRONE, W.C. (1973): *The Particle Atlas: an Encyclopedia of Techniques for Small Particle Identification I*. Ann Arbor Science Publishers, Ann Arbor, Michigan.
- MURRAY, J.A. (1979): Iron oxides. In *Marine Minerals* (R. Burns, ed.). *Rev. Mineral.* **6**, 47-98.
- PARFITT, R. L., VAN DER GAAST, S.J. & CHILDS, C.W. (1992): A structural model for natural siliceous ferrihydrite. *Clays Clay Minerals* **40**, 675-681.
- PEACOR, D.R. (1992): Analytical electron microscopy: X-ray analysis. In *Minerals and Reactions at the Atomic Scale: Transmission Electron Microscopy* (P.R. Buseck, ed.). *Rev. Mineral.* **27**, 113-140.
- RUSSELL, J.D. (1979): Infrared spectroscopy of ferrihydrite: evidence for the presence of structural hydroxyl groups. *Clay Mineral.* **14**, 109-113.

- SCHWERTMANN, U. & CORNELL, R.M. (1991): *Iron Oxides in the Laboratory: Preparation and Characterization*. VCH Publishers, Inc., New York, N.Y.
- SCOTT, S.D., CHASE, R.L., HANNINGTON, M.D., MICHAEL, P.J., MCCONACHY, T.F. & SHEA, G.T. (1990): Sulphide deposits, tectonics and petrogenesis of Southern Explorer Ridge, northern Pacific Ocean. In *Ophiolites: Oceanic Crustal Analogues*, Proc. "Troodos 1987" Symp. (J. Malpas, E.M. Moores, A. Panayiotou & C. Xenophontos, eds.). Geol. Surv. Dep., Ministry Agriculture Nat. Resources, Nicosia, Cyprus (719-733).
- STOFFERS, P., GLASBY, G.P., STUBEN, D., RENNER, R.M., PIERRE, T.G., WEBB, J. & CARDILE, C.M. (1993): Comparative mineralogy and geochemistry of hydrothermal Fe-rich crusts from the Pitcairn, Teahitea-Meheta, and Macdonald hot spot areas of the S.W. Pacific. *Marine Georesources Geotechnol.* **11**, 45-86.
- _____, SINGER, A., MCMURTRY, G., ARQUIT, A. & YEH, HSUEH-WEN (1990): Geochemistry of a hydrothermal nontronite deposit from the Lau Basin, Southwest Pacific. In *Geological Evolution and Hydrothermal Activity in the Lau and North Fiji Basins*, Results of SONNE Cruise 5035 (U. Stackelberg & U. von Rad, eds.). Roco-Druck GmbH, Wolfenbittel, Hannover, Germany (615-628).
- TOWE, K.M. & BRADLEY, W.F. (1967): Mineralogical constitution of colloidal "hydrous ferric oxides". *J. Colloid Interface Sci.* **24**, 384-392.
- TUNNICLIFFE, V., BOTROS, M.E., DE BURGH, D.A. JOHNSON, H.P., JUNIPER, S.K. & MCDUFF, R.E. (1986): Hydrothermal vents of Explorer Ridge, northeast Pacific. *Deep Sea Research* **33A**, 401-412.
- VAN DER GIESSEN, A.A. (1966): The structure of iron oxide-hydrate gels. *J. Inorg. Nucl. Chem.* **28**, 2155-2159.
- VEMPATI, R.K. & LOEPPERT, R.H. (1989): Influence of structural and adsorbed Si on the transformation of synthetic ferrihydrite. *Clays Clay Minerals* **37**, 273-279.
- VON STACKELBERG, U., MARCHIG, V., MULLER, P. & WEISER, T. (1990): Hydrothermal mineralization in the Lau and North Fiji basins. In *Geological Evolution and Hydrothermal Activity in the Lau and North Fiji Basins*, Results of SONNE Cruise S0-35 (U. von Stackelberg & U. von Rad, eds.). Roco-Druck GmbH, Wolfenbittel, Hannover, Germany (547-614).
- WAYCHUNAS, G.A. (1991): Crystal chemistry of oxides and oxyhydroxides. In *Oxide Minerals: Petrologic and Magnetic Significance* (D.H. Lindsley, ed.). *Rev. Mineral.* **25**, 11-68.
- WILLIAMS, D.B. (1984): *Practical Analytical Electron Microscopy in Materials Science*. Philips Electronic Instruments Inc., Electron Optics Publishing Group, Mahwah, New Jersey.
- ZHAO, JIANMIN, HUGGINS, F.E., FENG, ZHEN & HUFFMAN, G.P. (1994): Ferrihydrite: surface structure and its effects on phase transformation. *Clays Clay Minerals* **42**, 737-746.

Received January 5, 1998, revised manuscript accepted June 12, 1999.